Journal of Breath Research

PAPER

Real-time breath analysis of exhaled compounds upon peppermint oil ingestion by secondary electrospray ionization-high resolution mass spectrometry: technical aspects

Amanda Gisler[1], Jiayi Lan[2], Kapil Dev Singh[1,3], Jakob Usemann[1], Urs Frey[1,3], Renato Zenobi[2] and Pablo Sinues[1,3,4]

[1] University Children's Hospital Basel, Basel, Switzerland
[2] Department of Chemistry and Applied Biosciences, ETH Zurich, Zurich, Switzerland
[3] Department of Biomedical Engineering, University of Basel, Basel, Switzerland
[4] Author to whom any correspondence should be addressed.

E-mail: pablo.sinues@unibas.ch

Keywords: breath analysis, real-time mass spectrometry, peppermint oil

Supplementary material for this article is available online

OPEN ACCESS

RECEIVED
20 January 2020

REVISED
18 June 2020

ACCEPTED FOR PUBLICATION
23 June 2020

PUBLISHED
16 July 2020

Abstract

Breath analysis by secondary electrospray ionization high-resolution mass spectrometry (SESI-HRMS) has potential for clinical diagnosis and drug monitoring. However, there is still a lack of benchmarking data that shows the capability of this technique and allows comparability with other breath analysis techniques. In this regard, the goal of this study was the identification of volatile compounds upon ingestion of a specific peppermint oil capsule to get benchmark data for real-time breath analysis with SESI-HRMS. This was done in the framework of a consortium set up by the International Association of Breath Research (IABR), aimed at comparing several analytical instruments for breath analysis.

Breath temporal profiles of two subjects were analyzed with SESI-HRMS before and after ingestion of a peppermint oil capsule. The measurements were performed at two different locations using identical SESI-HRMS platforms to allow for comparability and benchmarking. Remarkably, along with the four major compounds (monoterpenes/cineole, menthone, menthofuran and menthol) reported by other members of the consortium, we detected 57 additional features significantly associated ($\rho > 0.8$) with the peppermint oil capsule, suggesting that this relatively simple intervention might trigger a more complex metabolic cascade than initially expected. This observation was made on both sites. Additional replicate experiments for one of the subjects suggested that a core of 35–40 unique molecules are consistently detected in exhaled breath upon ingestion of the capsule. In addition, we illustrate the analytical capabilities of real-time SESI-HRMS/MS to assist in the identification of unknown compounds. The results outlined herein showcase the performance of SESI-HRMS and enable comparison with other breath analysis techniques. Along with that, they strengthen the potential of this analytical technique for non-invasive drug monitoring and clinical diagnostic purposes.

1. Introduction

Breath analysis by mass spectrometry has promising potential for clinical diagnosis and non-invasive drug monitoring [1]. To date, several highly sensitive analytical techniques exist for the detection of volatile organic compounds (VOCs) in exhaled breath. These include gas chromatography-mass spectrometry (GC-MS) [2], proton-transfer-reaction mass spectrometry (PTR-MS) [3], selected-ion flow-tube mass spectrometry (SIFT-MS) [4] and ion mobility spectrometry (IMS) [5]. Recently, secondary electrospray ionization high-resolution mass spectrometry (SESI-HRMS) has evolved as a novel breath analysis technique. In contrast to PTR-MS and SIFT-MS, ionization of gas-phase species in SESI-HRMS takes place at atmospheric pressure [6], enabling its interfacing with commercial ultra-high-resolution mass

spectrometers (Res > 100 000). This allows a great deal of metabolic information to be captured in real-time, as such high resolutions facilitate zooming-in to minor species of low volatility that would otherwise be buried under the MS peaks of the most volatile (abundant) species [7, 8].

Despite the attractiveness of SESI-HRMS for breath metabolomics, just a handful of research groups are active in this field [9–17]. In order to facilitate intergroup data comparison, a series of instrumental upgrades and procedures to standardize breath analysis by SESI-HRMS have been recently developed [18]. Most relevant is the introduction of an exhalation interface (Exhalion, FIT, Spain) allowing real-time readout of critical exhalation parameters such as CO_2, exhaled volume and exhalation flow rate in parallel to the MS read-out. Additionally, disposable bacterial filters are now used as standard mouthpieces. Benchmarking data for breath analysis with SESI-HRMS remain scarce, and across other techniques data is even rarer. In order to address this issue, we present data acquired at two different sites incorporating these new gadgets and procedures. Moreover, we do so under the umbrella of the so-called 'Peppermint Consortium', which is a task force created at the International Association of Breath Research (IABR) aiming to benchmark the performances of different analytical instruments used for the same intervention—VOCs of peppermint oil monitored in exhaled breath after ingestion of a peppermint oil capsule. Comparability among the different instruments of all the participating research groups is ensured by the use of peppermint oil capsules from the same company and manufacturing batch.

2. Material and methods

2.1. Subjects and measurement procedure

The experiments presented here were conducted in accordance with the Declaration of Helsinki. The protocol in this study was approved by the local Ethics Committees (Ethics Committee for Northwest and Central Switzerland 2018–01324; Ethics Commission of ETH Zurich EK 2018-N-70). Two healthy female subjects (26 years, 35 years) from two sites (ETH Zurich and University Children's Hospital Basel) were recruited and informed consent was obtained before enrollment. In both sites a standardized protocol and identical equipment was used. To reduce confounding by species from exogenous origin other than peppermint oil, the subjects were asked to fast and abstain from chewing gum or brushing their teeth for at least 1 h prior to the measurements. Both subjects provided a baseline breath sample in positive and negative mode 30 min before ingestion of a 200-mg peppermint oil capsule (Boots, Nottingham, UK). Subsequent breath samples (14 per subject) were measured at 0, 30, 60, 90, 165, 285 and 360 min after capsule ingestion. For each time point, 10 replicate exhalations were separately acquired in positive and negative ionization mode. To reduce variation in capsule thickness and concentration of volatile compounds in the capsule, we used capsules from the same batch (batch number 200 207) as other research groups within the Peppermint Consortium. Nonetheless, a small variability in the contents of the capsules can be expected [19].

2.2. Instrumentation and chemicals

The analytical platform consisted of an exhalation interface (Exhalion, FIT, Spain) for real-time display of CO_2, flow rate and exhaled volume, and an ion source (Super SESI, FIT, Spain) coupled to a high-resolution mass spectrometer (Q-Exactive Plus, Thermo Fisher Scientific, Germany). Commercially available bacterial filters (MicroGard, Vyaire Medical, USA) were used as mouthpieces. Mass spectra were acquired in full scan mode over the mass range m/z 70–400 with a resolution of 140 000 for positive and 70 000 for negative mode at m/z 200. MS settings included 2 microscans, automatic gain control (AGC) target of 1×10^6 and maximum injection time of 500 ms. Real-time SESI-HRMS/MS fragmentation experiments of peppermint oil compounds in breath and chemical standards were performed using collision-induced dissociation (CID) by varying normalized collision energy (15%, 20%, 30% and 50%). Similarity scores for MS/MS spectra of breath vs chemical standards were computed by calculating the cosine of the angle between the two vectors (dot product divided by the product of their lengths). Hence the score lies between 1 (maximum similarity) and 0 (minimum similarity). Additionally, in-source fragmentation patterns in full MS mode were examined for several chemical standards of typical peppermint compounds. All chemical standards were purchased from Sigma-Aldrich (Merck) and had a purity $\geq$ 90% (Electronic Supplementary Material (ESM) table S1, available at stacks.iop.org/JBR/14/046001/mmedia).

For the electrospray formation, a 20-µm inner diameter (ID) non-coated TaperTip silica capillary emitter (New Objective, Woburn, MA) and 0.1% formic acid in water were used. The Super SESI solvent reservoir pressure was set to 1.3 bar. The temperature of the ionization chamber was set to 90 °C and the sampling line temperature was set to 130 °C. The set point of the exhaust mass flow controller was 0.7 l/min and nitrogen mass flow through the source was 0.4 l/min to ensure a constant fraction of breath entering the ionizer (0.3 l/min).

2.3. Data analysis: pre-processing

Data pre-processing and statistical analyses were performed using MATLAB (version 2019a and 2019b, MathWorks Inc., USA). Briefly, raw data from the MS was converted to mzXML format with msConvert (ProteoWizard) [20]. Peaks with a signal intensity

above 10^4 a.u. in Thermo's signal intensity scale, were selected for further analysis. Then, exhalation time windows were defined by CO_2 concentrations above 3% (as measured by Exhalion). Subsequently, the correlation coefficient of all ion time traces with the CO_2 time trace were computed. Ion signals with a correlation coefficient of at least 0.6 (i.e. mirroring CO_2) were considered breath-related and used for the next steps. The area under the curve (AUC) for each mass spectral feature during the exhalation windows was computed using trapezoidal numerical integration. These AUCs were then normalized by the exhalation time and the 10 replicate normalized AUCs for each feature were averaged afterwards. For the final data matrix only features present in at least 30% of the samples were considered.

2.4. Data analysis: post-processing

Features with a typical washout profile were selected by identifying those that correlated with the monoterpene ion (i.e. $[C_{10}H_{17}]^+$). This ion has been shown to be a clear washout product upon peppermint oil ingestion [19, 21], and hence was used as the reference compound. Because the time traces could peak at different time points, they were previously aligned to the monoterpene by computing the cross-correlations between the pairs of signals and the monoterpene. After alignment, Pearson's linear correlation coefficients (ρ) between all traces and terpene, along with corresponding p-values were computed. Furthermore, we estimated a positive false discovery rate (FDR) for multiple hypothesis testing using the procedure introduced by Benjamini and Hochberg [22]. We then considered features with a correlation $\rho > 0.8$ and time-to-peak between 30–360 min after capsule ingestion. Peaks before 30 min were not considered, as they might be related to reflux of stomach gases containing high levels of volatile compounds of peppermint oil [21]. Subsequently, we generated molecular formulae for this reduced list of ions mirroring the typical washout profile of monoterpene. Based on the accurate mass (typically within 1 ppm) and considering the elements C, H, N and O, molecular formulae were generated, using the so-called golden rules [23]. Furthermore, we compared the theoretical and experimental isotopic distributions to provide further evidence on the accuracy of the molecular formula assignment. Isotopes were subsequently removed from further analysis. Finally, according to the literature that characterizes volatile compounds of peppermint oil by GC-MS and PTR-MS, a list of tentative compounds for observed features was generated [19, 24–26]. For two compounds of interest (i.e. limonene-1,2-diol, p-cymene), we additionally conducted SESI-HRMS/MS fragmentation experiments of exhaled breath after intake of the peppermint oil capsule and compared the spectra with the corresponding chemical standard.

3. Results and discussion

The main goal of this study was to acquire benchmarking data for real-time breath analysis with SESI-HRMS. Following the recommendations of the IABR Peppermint Consortium, the initial benchmarking data that we present include the provision of a reference on the number of features to be expected when conducting real-time chemical analysis via SESI-Orbitrap. When applying the instrumentation settings outlined above (most critical are resolution and signal intensity threshold), one should expect to detect for one individual around 550 features in positive mode in the mass range 70–400 (ESM figure S1; resolution 140 000 and intensity threshold 10^4). The negative ion mode mass spectrum is typically less populated, with around 400 features to be expected (ESM figure S1: resolution 70 000 and intensity threshold 10^4). Observations of significant lower numbers of peaks in the breath mass spectra should signify a warning. It is again worth noting that SESI-HRMS has a unique ability to access in the order of 1000 mass spectral features in breath associated with human metabolism.

3.1. Monitoring of four main components: monoterpenes/cineole, menthone, menthofuran and menthol

Upon pre-processing of the raw data, we ended up with a data matrix of 16 samples (2 subjects x 8 time points) and 1408 features (904 features in positive mode and 504 features in negative mode) that were present in at least 30% of the breath samples. We initially performed a targeted approach by confirming that the four main components detected by another real-time mass spectrometric technique (i.e. PTR-MS) can also be identified with SESI-HRMS [19]. Figure 1(a) shows the washout profiles of the four compounds (monoterpenes/cineole, menthone, menthofuran, menthol) for the two subjects. The profiles are very similar to the ones already reported within the consortium [19]. These findings serve as first evidence that SESI-HRMS can provide comparable results to those of PTR-MS. Also, in-line with previous observations [21], we observed an individual variability in the time-to-peak. For example, the maximum signal intensity for *m/z* 137.1325 $[C_{10}H_{17}]^+$ in the subject at site 2 was approximately one hour later than in the subject from site 1. The same delayed time-to-peak could also be observed for a fragment of menthol $[C_{10}H_{19}]^+$ and menthone $[C_{10}H_{19}O]^+$, but not for menthofuran $[C_{10}H_{15}O]^+$. The variability in the washout profiles of exhaled volatile compounds of peppermint oil may result from varying speed in the capsule breakdown, absorption, age and BMI, but might also reflect individual metabolism [19]. A separate tandem manuscript investigates this aspect in depth in a larger cohort [29].

Malásková *et al* [19] reported on additional features assigned to fragments of monoterpenes/cineole, menthone, menthofuran and menthol when analyzing breath with PTR-MS. In-source fragmentation is an undesired phenomenon as it adds complexity to the spectra, compromising the interpretation of the results. Electrospray ionization and its variants such as SESI are regarded as gentle ionization methods because they produce low ion excitation and hence induce little or no fragmentation of the analyte. We investigated in-source fragmentation of some relevant compounds by analyzing in full-MS mode the headspace of chemical standards. We observed varying degrees of fragmentation from labile molecules such as α-pinene and limonene (both monoterpenes) to no fragmentation at all for piperitone and pulegone (ESM figures S2-S4).

3.2. Monitoring of other components

One of the main advantages of SESI-HRMS is its capability to combine high sensitivity of electrospray ionization [6, 27] with resolutions in excess of 100 000. This allows for the detection of typically ~1000 mass spectral features per individual in each experiment (ESM figure S1). For this reason, we further explored whether additional signals related to the peppermint oil capsule ingestion can be detected by our method. To do so, we computed the pairwise correlation coefficient (ρ) between each of the features and the monoterpene ion $[C_{10}H_{17}]^+$. One hundred and sixty features correlated ($\rho > 0.8$; FDR < 0.057) with this ion in the subject from site 1 (ESM table S2) whereas 197 features were found to be correlated ($\rho > 0.8$; FDR < 0.067) in the subject from site 2 (ESM table S3). Out of the 160 and 197 features, 90 were found in both subjects. This list was further reduced to 60 features after deisotoping (table 1). Temporal profiles for two examples of such molecules are shown in figure 1(b). They correspond to $[C_{10}H_{19}O_2]^+$ and $[C_{10}H_{15}]^+$. In the next section we describe the analytical capabilities of our breath analysis platform to identify these compounds. The majority of the features were detected in positive ion mode (i.e. 47), yet, more noteworthy is that 13 features were detected in negative ion mode. These are typically organic acids undergoing deprotonation. The high number of correlating features and the fact that some are detected in positive and some others in negative ion mode (i.e. metabolites with diverse chemical functionalities), provides a first indication that the peppermint oil consumption may induce a more complex metabolic response than initially thought, based on ongoing studies within the consortium. Further insights on the origins and biochemistry of these metabolites are presented in the accompanying paper from Lan *et al* [29].

Similar to what has been observed for the four main compounds of peppermint oil, we also found quite a variation in time-to-peak between the two subjects for the additionally identified features. Figure 2 shows that in both subjects the majority of features peak between 30–165 min after capsule ingestion. In general, it can be said that in the subject from site 1 most features peak earlier than in the subject from site 2. In subject 1 most of the features peak at 60 and 90 min after capsule ingestion whereas in subject 2 the majority of the features peak at 90 min after capsule ingestion but not before (figure 2 and ESM figure S5). Overall, these results were further confirmed in a series of replicate experiments, whereby one of the subjects repeated the experiment seven times. Forty nine out of 61 features were consistently detected within 1 ppm error. We also computed the pairwise-correlation across the 49 features for all replicate experiments (ESM figure S6 and the last two columns of table 1). We found that 28 ions did not correlate with any other ion ($\rho < 0.95$), placing a high confidence on these ions corresponding to unique molecules. The remaining 21 ions correlated with each other in eight different clusters, suggesting that these correspond to eight fairly labile molecules undergoing in-source fragmentation. For example, the correlation coefficient between m/z 177.1638 (i.e. $C_{13}H_{20}$) and 195.1743 (i.e. $C_{13}H_{22}O$) was 0.9505. Such high correlation and their molecular formulae suggest that $C_{13}H_{20}$ is the result of a loss of water of $C_{13}H_{22}O$ (cluster 'h' in table 1) during in-source fragmentation. This analysis leads us to the conclusion that, after removing redundant features such as isotopes and fragments, SESI-HRMS breath analysis allows for the real-time monitoring of 35–40 unique molecules during this intervention. The temporal profiles of these molecules across the additional replicate measurements were largely reproducible, although some variability in the time-to-peak was observed, suggesting that the intra-subject variability is indeed non-negligible (ESM figure S6).

3.3. Compound identification: isotopic distribution, kendrick plots and collision induced dissociation

One of the shortcomings of real-time analytical mass spectrometric platforms is the remaining challenge in compound identification, since no chromatographic separations exist upstream. Hence, all the separation power relies on the MS resolution. In the following section, we describe the strategy developed to gain more insights into the features reported in table 1 and how they could potentially be linked to peppermint oil ingestion.

The first step was to produce a list of feasible molecular formulae that matched the experimental mass within 1 ppm. In some cases, especially for masses larger than 100 Da, there can be several candidate formulae, even within such a narrow mass error window. Therefore, we compared

Table 1. Features identified in exhaled breath via SESI-HRMS stemming from peppermint oil ingestion.

						Subject/Site 1				Subject/Site 2					
m/z	Adduct	Molecular Formula	Name (tentative identification)[b]	RDBE	Mass error (ppm)	Time-to-Peak	ρ	p-val	FDR	Time-to-Peak	ρ	p-val	FDR	Detected in rep. exp.[c]	Cluster[d]
77.03792	[M + H] +	unassignable		–	–	60 min	0.899	1E-07	0.021	90 min	0.999	6E-09	8E-07	No	–
77.03853	[M + H] +	C_6H_4	menthofuran fragment, alkyl fragment	5	−0.613	30 min	1.000	4E-12	2E-09	90 min	0.999	4E-10	9E-08	Yes	a
79.05421	[M + H] +	C_6H_6	limonene fragment, benzene	4	−0.213	30 min	1.000	3E-09	2E-09	90 min	0.999	9E-10	2E-07	Yes	a
81.06988	[M + H] +	C_6H_8	1,3-cyclohexadiene, terpenes fragment	3	0.042	30 min	0.999	2E-10	4E-07	90 min	1.000	5E-12	2E-09	Yes	a
82.0761	[M + H] +	unassignable		–	–	30 min	1.000	0.012	4E-08	90 min	0.999	4E-09	6E-07	Yes	a
83.07654	[M + H] +	unassignable		–	–	30 min	1.000	0.010	2E-09	90 min	1.000	3E-11	8E-09	Yes	a
83.08549	[M + H] +	C_6H_{10}	hexenol fragment, menthol fragment	2	−0.446	60 min	0.823	0.013	0.048	90 min	0.951	3E-04	0.008	Yes	–
93.06989	[M + H] +	C_7H_8	terpene fragments	4	0.146	60 min	0.928	1E-08	0.013	90 min	0.943	4E-04	0.009	Yes	b
95.04913	[M + H] +	C_6H_6O[a]		4	−0.119	30 min	0.993	0.013	7E-05	90 min	0.984	1E-05	0.001	Yes	c
95.08552	[M + H] +	C_7H_{10}	terpene fragments	3	−0.070	30 min	0.999	0.009	9E-07	90 min	0.998	3E-08	3E-06	Yes	a
96.05247	[M + H] +	unassignable		–	–	30 min	0.992	0.013	1E-04	90 min	0.979	2E-05	0.001	Yes	c
105.0369	[M + H] +	unassignable		–	–	285 min	0.858	4E-04	0.036	360 min	0.941	5E-04	0.010	Yes	–
107.0855	[M + H] +	C_8H_{10}	2-ethenylbicyclo[2.1.1]hex-2-ene, ethylbenzene	4	−0.156	60 min	0.908	0.010	0.018	90 min	0.874	0.005	0.035	Yes	b
110.0726	[M + H] +	unassignable		–	–	60 min	0.881	0.001	0.026	90 min	0.865	0.006	0.038	Yes	d
111.1168	[M + H] +	C_8H_{14}		2	−0.060	30 min	0.842	0.006	0.041	90 min	0.942	5E-04	0.009	Yes	–
113.0961	[M + H] +	$C_7H_{12}O$	2-methylcyclohexanone	2	−0.189	90 min	0.887	0.015	0.024	90 min	0.969	7E-05	0.003	Yes	–
116.0116	[M − H]−	unassignable		–	–	165 min	0.826	0.001	0.047	360 min	0.841	0.009	0.048	Yes	–
123.1169	[M + H] +	C_9H_{14}	sesquiterpene fragments	3	0.192	60 min	0.900	0.003	0.021	90 min	0.817	0.013	0.059	Yes	–
125.0972	[M − H]−	$C_8H_{14}O$	sulcatone	2	0.095	90 min	0.825	0.002	0.047	90 min	0.931	0.001	0.012	Yes	–
133.1012	[M + H] +	$C_{10}H_{12}$	menthofuran fragment, p-cymenene	5	0.177	60 min	0.932	0.002	0.012	90 min	0.878	0.004	0.033	Yes	–
135.1168	[M + H] +	$C_{10}H_{14}$	p-cymene	4	0.100	60 min	0.828	0.004	0.047	90 min	0.940	0.001	0.010	Yes	b
136.1246	[M + H] +	unassignable		–	–	60 min	0.884	0.001	0.025	90 min	0.847	0.008	0.045	Yes	–
137.0792	[M + H] +	unassignable		–	–	285 min	0.918	0.011	0.015	90 min	0.988	4E-06	2E-04	No	–
137.0805	[M + H] +	unassignable		–	–	90 min	0.835	0.001	0.044	90 min	0.979	2E-05	0.001	No	–
137.1156	[M + H] +	unassignable		–	–	30 min	0.997	0.005	7E-06	90 min	0.993	9E-07	7E-05	No	–
137.1325	[M + H] +	$C_{10}H_{16}$	limonene, pinene	3	−0.122	90 min	Ref	Ref	Ref	90 min	Ref	Ref	Ref	Yes	e
137.1493	[M + H] +	unassignable		–	–	30 min	0.996	7E-08	1E-05	90 min	0.990	2E-06	2E-04	No	–
137.1849	[M + H] +	Unassignable		–	–	90 min	0.893	0.003	0.022	90 min	0.989	3E-06	2E-04	No	–
139.142	[M + H] +	unassignable		–	–	30 min	0.998	0.009	3E-06	90 min	0.995	3E-07	3E-05	Yes	e
139.1481	[M + H] +	$C_{10}H_{18}$	menthol fragment, cis-sabinene hydrate	2	−0.265	60 min	0.811	2E-11	0.053	90 min	0.954	2E-04	0.007	Yes	–
149.0961	[M + H] +	$C_{10}H_{12}O$	menthofuran fragment	5	0.262	90 min	0.864	0.001	0.033	90 min	0.814	0.014	0.059	Yes	–

(Continued)

Table 1. (Continued).

						Subject/Site 1				Subject/Site 2					
m/z	Adduct	Molecular Formula	Name (tentative identification)[b]	RDBE	Mass error (ppm)	Time-to-Peak	ρ	p-val	FDR	Time-to-Peak	ρ	p-val	FDR	Detected in rep. exp.[c]	Cluster[d]
150.1039	[M + H] +	unassignable		–	–	60 min	0.980	0.015	0.001	90 min	0.861	0.006	0.040	Yes	f
151.1118	[M + H] +	$C_{10}H_{14}O$	menthofuran, carvone	4	0.125	90 min	0.940	0.002	0.010	90 min	0.916	0.001	0.018	Yes	–
153.1274	[M + H] +	$C_{10}H_{16}O$	pulegone, piperitone	3	−0.074	60 min	0.876	0.004	0.028	90 min	0.972	5E-05	0.002	Yes	–
154.1352	[M + H] +	unassignable		–	–	60 min	0.968	0.001	0.003	90 min	0.955	2E-04	0.007	Yes	–
155.143	[M + H] +	$C_{10}H_{18}O$	menthone, 1,8-cineole	2	−0.138	60 min	0.926	3E-04	0.014	90 min	0.994	5E-07	5E-05	Yes	–
163.0251	[M − H]−	unassignable		–	–	90 min	0.827	0.004	0.047	360 min	0.807	0.015	0.064	No	–
165.0922	[M − H]−	$C_{10}H_{14}O_2$		4	0.707	90 min	0.861	0.001	0.034	90 min	0.857	0.007	0.041	Yes	g
166.0989	[M + H] +	unassignable		–	–	90 min	0.956	0.010	0.006	90 min	0.894	0.003	0.027	Yes	f
167.1067	[M + H] +	$C_{10}H_{14}O_2$	mintlactone, perillic acid	4	0.085	90 min	0.952	8E-05	0.007	90 min	0.907	0.002	0.021	Yes	–
168.1145	[M + H] +	unassignable		–	–	60 min	0.946	0.002	0.009	90 min	0.848	0.008	0.045	Yes	d
169.1223	[M + H] +	$C_{10}H_{16}O_2$	(-)-(Z)-Tetrahydro-6-(2-pentenyl)-2 H-pyran-2-one	3	0.025	60 min	0.839	0.017	0.042	90 min	0.894	0.003	0.026	Yes	–
170.154	[M + H] +	$C_{10}H_{19}ON$[a]		2	0.058	30 min	0.992	0.004	1E-04	90 min	0.951	3E-04	0.008	yes	–
171.1379	[M + H] +	$C_{10}H_{18}O_2$	menthone lactone, limonene-1,2-diol	2	−0.093	60 min	0.820	3E-04	0.049	90 min	0.942	5E-04	0.009	yes	–
172.1696	[M + H] +	$C_{10}H_{21}ON$		1	−0.118	30 min	0.980	0.001	0.001	90 min	0.966	1E-04	0.004	yes	–
173.0093	[M − H]−	$C_6H_6O_6$		4	0.799	90 min	0.846	0.003	0.040	30 min	0.877	0.004	0.034	yes	–
177.1638	[M + H] +	$C_{13}H_{20}$	heptylbenzene	4	−0.094	165 min	0.923	0.002	0.014	90 min	0.915	0.001	0.018	yes	h
181.0872	[M − H]−	$C_{10}H_{14}O_3$	peperinic acid	4	0.894	90 min	0.831	0.001	0.046	90 min	0.814	0.014	0.059	yes	g
182.0937	[M + H] +	unassignable		–	–	90 min	0.953	0.001	0.007	90 min	0.845	0.008	0.045	no	–
188.1645	[M + H] +	$C_{10}H_{21}O_2$ N		1	−0.239	30 min	0.844	0.007	0.041	90 min	0.860	0.006	0.040	yes	–
195.1743	[M + H] +	$C_{13}H_{22}O$	geranylacetone	3	−0.109	165 min	0.934	0.007	0.012	90 min	0.954	2E-04	0.007	yes	h
199.0964	[M + H] +	$C_{10}H_{14}O_4$[a]		4	−0.278	90 min	0.935	0.001	0.011	90 min	0.929	0.001	0.013	yes	–
205.1951	[M + H] +	$C_{15}H_{24}$	caryophyllene	4	−0.130	90 min	0.829	2E-04	0.046	165 min	0.898	0.002	0.025	yes	–
235.1414	[M + H] +	$C_9H_{14}N_8$[a]		7	−0.165	60 min	0.829	0.012	0.046	90 min	0.833	0.010	0.052	yes	–
253.181	[M − H]−	$C_{15}H_{26}O_3$		3	0.326	165 min	0.805	0.010	0.055	165 min	0.826	0.012	0.055	yes	–
299.1496	[M − H]−	unassignable		–	–	90 min	0.850	0.002	0.038	165 min	0.884	0.004	0.030	no	–
299.1857	[M − H]−	unassignable		–	–	90 min	0.838	0.003	0.043	165 min	0.887	0.003	0.029	yes	–
313.1651	[M − H]−	unassignable		–	–	90 min	0.835	0.002	0.044	165 min	0.862	0.006	0.040	no	–
315.1799	[M − H]−	$C_{13}H_{20}N_{10}$		9	−0.201	90 min	0.868	1E-04	0.031	165 min	0.913	0.002	0.018	no	–
317.1956	[M − H]−	$C_{13}H_{22}N_{10}$		8	0.021	90 min	0.860	0.005	0.034	165 min	0.858	0.006	0.041	no	–
331.1751	[M − H]−	$C_{13}H_{20}ON_{10}$[a]		9	0.548	90 min	0.858	0.002	0.036	165 min	0.877	0.004	0.034	yes	–

[a]Formula based on accurate mass only (not passing the matching threshold of theoretical isotopic pattern)

[b]Tentative compound based on matches in the literature

[c]yes = molecule detected (within 1 ppm) in at least one of the six additionally repeated experiments

[d]a-h = clusters of ions correlating with each other ($\rho > 0.95$)

RDBE = Ring double bond equivalent

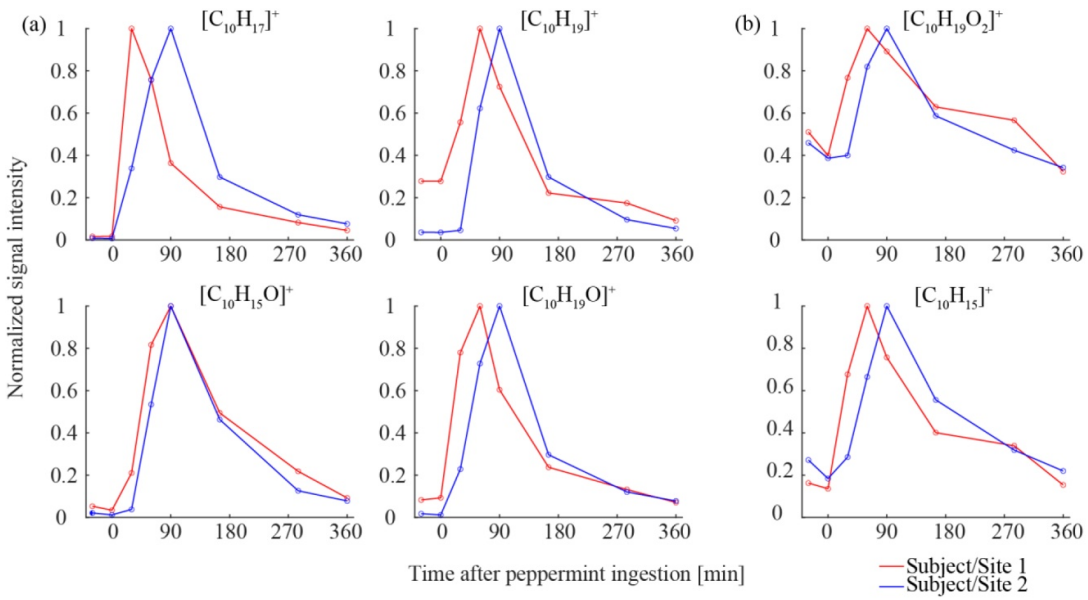

Figure 1. Secondary electrospray ionization high-resolution mass spectrometry (SESI-HRMS) detects previously reported compounds, but also reveals unreported exhaled molecules upon peppermint oil intake. Temporal profiles of normalized signal intensities: (a) typical peppermint compounds previously reported in breath as measured by other techniques [19]: $[C_{10}H_{17}]^+$ (monoterpenes + fragment of cineole), $[C_{10}H_{19}]^+$ (fragment of menthol), $[C_{10}H_{15}O]^+$ (menthofuran), $[C_{10}H_{19}O]^+$ (menthone); **(b)** features detected in breath associated with peppermint oil ingestion newly reported in this work: $[C_{10}H_{19}O_2]^+$ (limonene-1,2-diol), $[C_{10}H_{15}]^+$ (p-cymene).

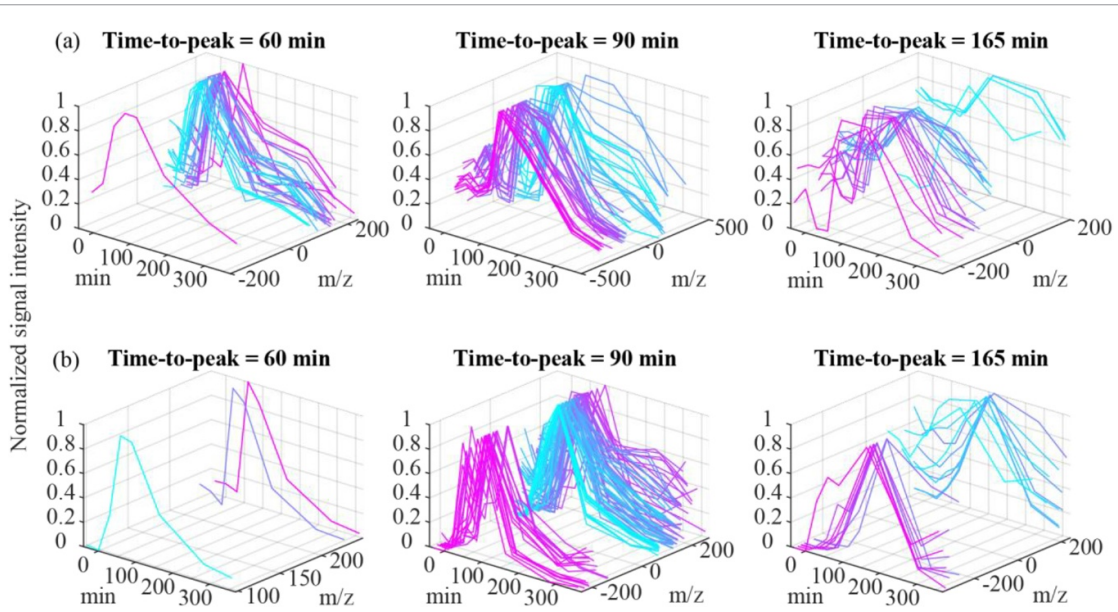

Figure 2. Overview of the richness of the metabolic signature captured by SESI-HRMS upon peppermint oil ingestion. Temporal profiles of features significantly correlating in at least one subject with time-to-peak at 60, 90 or 165 min after ingestion of the peppermint oil capsule (m/z with a negative sign correspond to ions detected in negative ionization mode; colors are only meant to ease visualization). (a) Most of the features (86 out of 161) in the subject from site 1 peak between 60 and 90 min after capsule ingestion. (b) In subject 2, most of the observed features (103 out of 198) peak 90 min after capsule ingestion.

the theoretical isotopic distribution of the candidate formulae with the measured mass spectra to narrow down the number of assigned formulae. Unless otherwise indicated, all molecular formulae listed in table 1 were obtained by combining their accurate mass and matching with the theoretical isotopic distribution, hence we place high confidence in these assignments. In figure 3 we show an example: the simulated isotopic distribution vs the experimental isotopic distribution for the monoterpene ion and the nearly perfect match of the peak location and peak intensity.

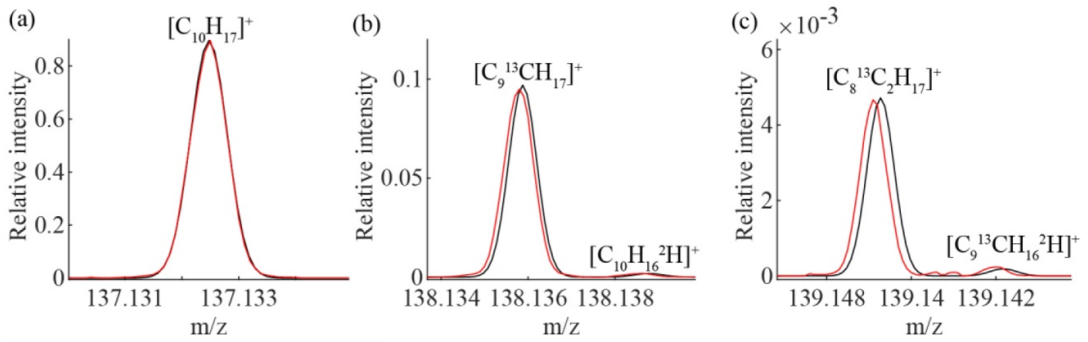

Figure 3. High mass accuracy and the detection of fine isotopic structures at ultra-high resolution enable unambiguous molecular formula assignment of exhaled compounds. Simulated isotopic distributions (black) were compared against experimental isotopic distributions (red) for the monoterpene ion. (a) Mass spectra of the protonated monoisotopic mass *m/z* 137.1325 ($[C_{10}H_{17}]^+$). (b) Mass spectra of the ^{13} C and the deuterium ^{2} H isotopes, (c) Mass spectra of the even smaller isotopes $[C_8{}^{13}C_2H_{17}]^+$ and $[C_9{}^{13}CH_{16}{}^{2}H]^+$ that are observable due to the high resolution.

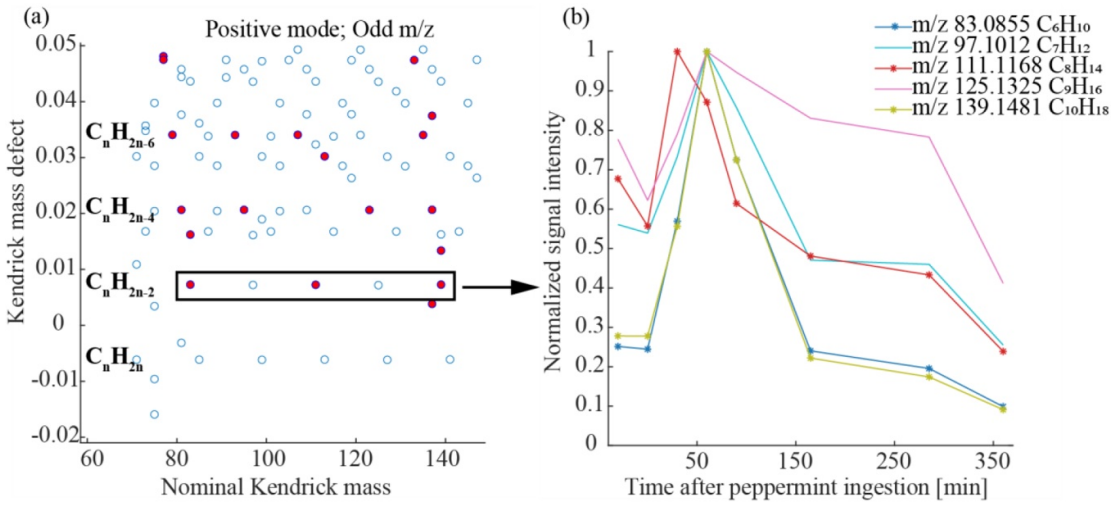

Figure 4. Simplification of the high-resolution complexity and identification of metabolite homologous series associated with peppermint oil metabolism. (a) Kendrick plot: Kendrick mass defect vs nominal Kendrick mass for odd-mass of all positive ions (blue dots) and of positive ions significantly correlated ($\rho > 0.8$) with $[C_{10}H_{17}]^+$ (red dots). (b) Similar washout profiles can be observed in subject/site 1 for significantly (connecting lines with star) correlated features ($[C_6H_{11}]^+$, $[C_8H_{15}]^+$, $[C_{10}H_{19}]^+$) and non-significantly correlated features ($[C_7H_{13}]^+$, $[C_9H_{17}]^+$) belonging to the same homologous series.

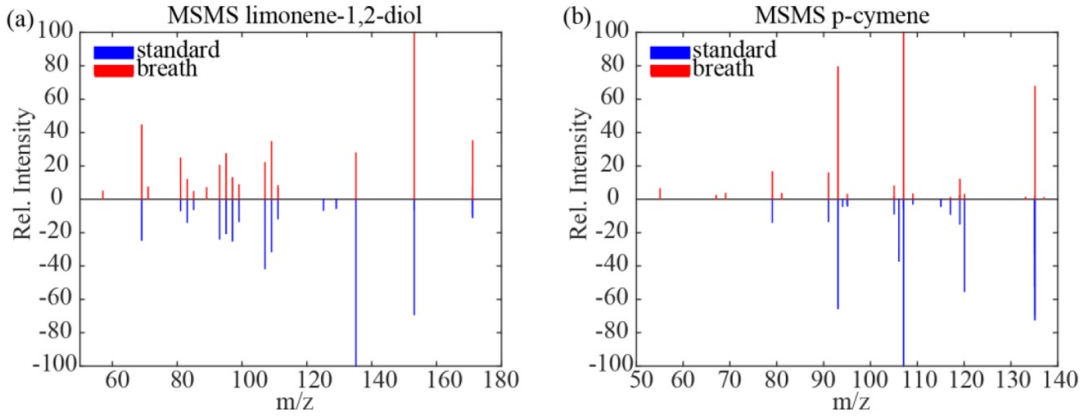

Figure 5. Real-time SESI-MS/MS for compound identification. (a) MS/MS spectrum of chemical standard (blue) suggests that *m/z* 171 observed in breath (red) is limonene-1,2-diol. (b) MS/MS spectrum of chemical standard (blue) suggests that *m/z* 135 observed in breath (red) is p-cymene.

To gain further insights into the relationships across the features listed in table 1 and their potential role in the peppermint oil metabolism, we plotted them using Kendrick's mass defect [28]. Kendrick plots assist in simplification of the complexity of high-resolution mass spectra, as they allow for the mapping and, in this case, localization of complete families of metabolites. Figure 4(a) shows a zoom of a Kendrick plot whereby homologous -CH_2- series of hydrocarbons with an increasing number of unsaturations are clearly observed (e.g. C_nH_{n-2}). Interestingly, several series were found where a high number of features correlated significantly ($\rho > 0.8$) with $[C_{10}H_{17}]^+$ (i.e. had a washout-like profile), for example $[C_6H_{11}]^+$, $[C_8H_{15}]^+$ and $[C_{10}H_{19}]^+$ ($[C_7H_{13}]^+$ and $[C_9H_{17}]^+$ correlated below the 0.8 threshold). This suggests that actually the complete metabolism of compound classes can be monitored. Figure 4(b) illustrates this by showing the time profiles of the C_nH_{n-2} series for one subject. Clearly, all the compounds in the series seem to be related to the peppermint metabolism. However, it should be noted that one limitation of SESI-HRMS is that it cannot resolve isomers. The confirmation of the hypothesis that these series of compounds actually relate to the same chemical families, would require further investigation.

Finally, we illustrated the compound identification capabilities of SESI-HRMS by attempting the identification of two compounds correlating with $[C_{10}H_{17}]^+$ by exploiting the SESI-HRMS/MS capabilities of the Q-Exactive Plus mass spectrometer. In particular, we concentrated on *m/z* 171.1379 and *m/z* 135.1168, which correspond to formulae $[C_{10}H_{19}O_2]^+$ and $[C_{10}H_{15}]^+$ (compounds shown in figure 1(b)). We hypothesized that these compounds correspond to limonene-1,2-diol (a metabolite of limonene) and p-cymene (a minor volatile constituent of peppermint oil). We performed MS/MS experiments on the pure chemical standards of these compounds to compare the fragmentation patterns with those obtained in breath. Figure 5(a) shows the CID MS/MS spectrum of *m/z* 171 (isolation window 1 Da) as exhaled in real-time compared to the MS/MS spectrum of the chemical standard of limonene-1,2-diol. The similarity of the spectra (match score 0.73, where 1 = max similarity; ESM table S4) supports the hypothesis that the molecule could indeed be limonene-1,2-diol. Figure 5(b) shows the CID MS/MS spectrum of *m/z* 135 (isolation window 1 Da) that is very similar to the spectrum of the chemical standard of p-cymene (match score 0.78, ESM table S4). This increases our confidence that the molecule we see in breath is actually p-cymene.

4. Conclusions

We have showcased the analytical capabilities of SESI-HRMS/MS to monitor exhaled compounds in real-time in the context of the 'Peppermint Consortium'. Key features of our analytical platform include low limits of detection (ppt range), mass resolutions in excess of 100 000, mass accuracies within 1 ppm, the possibility of positive and negative mode ionization and collision-induced dissociation capabilities [27]. Such outstanding analytical figures of merit allowed us to unveil around 60 features (estimated 35–40 unique molecules) associated with peppermint oil ingestion in two subjects, providing unprecedented insights for the consortium. The accompanying manuscript of Lan *et al* [29] confirms that most of these molecules are indeed detectable in multiple independent measurements of several subjects. Some of them are thought to be linked to menthol and limonene metabolism, for example cis/trans-carveol and limonene-1,2-diol. Further comprehensive characterization of the entire panel of the reported molecules is still required. However, we expect that the reported accurate *m/z* values and associated molecular formulae will sufficiently enhance the impact of the consortium on the provision of a comprehensive overview of metabolic changes triggered by ingestion of peppermint oil capsule. Overall, the results presented here reinforce the notion of the outstanding potential of SESI-HRMS for non-invasive drug-monitoring and clinical diagnostic purposes.

Acknowledgments

This study has been conducted under the framework of the 'Peppermint Consortium' founded by Paul Thomas (Loughborough University, UK), Simona Cristescu (Radboud University, Netherlands), Jonathan Beauchamp (Fraunhofer Institute for Process Engineering and Packaging IVV, Germany) and Stephen Fowler (The University of Manchester, UK). We gratefully ackowledge this initiative. This work is also part of the Zurich Exhalomics project under the umbrella of The University of Medicine Zurich/*Hochschulmedizin Zürich.*

Funding

This study was funded by the Fondation Botnar, Switzerland (Professorship of Pablo Sinues) and the Swiss National Science Foundation (grant No. 320030_173168 and PCEGP3_181300).

ORCID iDs

Amanda Gisler https://orcid.org/0000-0002-9708-1200
Jiayi Lan https://orcid.org/0000-0002-2278-0779
Kapil Dev Singh https://orcid.org/0000-0002-5682-0708
Renato Zenobi https://orcid.org/0000-0001-5211-4358

Pablo Sinues https://orcid.org/0000-0001-5602-2880

References

[1] Singh K D, Del Miguel G V, Gaugg M T, Ibañez A J, Zenobi R, Kohler M, Frey U and Sinues P M-L 2018 Translating secondary electrospray ionization-high-resolution mass spectrometry to the clinical environment *J. Breath Res.* **12** 027113

[2] Guallar-Hoyas C, Turner M A, Blackburn G J, Wilson I D and Thomas C P 2012 A workflow for the metabolomic/metabonomic investigation of exhaled breath using thermal desorption GC-MS *Bioanalysis* **4** 2227–37

[3] Trefz P, Schmidt M, Oertel P, Obermeier J, Brock B, Kamysek S, Dunkl J, Zimmermann R, Schubert J K and Miekisch W 2013 Continuous real time breath gas monitoring in the clinical environment by proton-transfer-reaction-time-of-flight-mass spectrometry *Anal. Chem.* **85** 10321–9

[4] Spanel P, Dryahina K and Smith D 2013 A quantitative study of the influence of inhaled compounds on their concentrations in exhaled breath *J. Breath Res.* **7** 017106

[5] Ruzsanyi V, Baumbach J I, Sielemann S, Litterst P, Westhoff M and Freitag L 2005 Detection of human metabolites using multi-capillary columns coupled to ion mobility spectrometers *J. Chromatogr.* A **1084** 145–51

[6] Rioseras A T, Gaugg M T and Sinues P M L 2017 Secondary electrospray ionization proceeds via gas-phase chemical ionization *Anal. Methods* **9** 5052–7

[7] Li H, Zhu J and Hill J E 2020 Secondary electrospray ionization mass spectrometry for breath studies *Encyclopedia of Analytical Chemistry: Applications, Theory and Instrumentation* ed R A Meyers pp 1–14

[8] Li X, Huang L, Zhu H and Zhou Z 2017 Direct human breath analysis by secondary nano-electrospray ionization ultrahigh-resolution mass spectrometry: importance of high mass resolution and mass accuracy *Rapid Commun. Mass Spectrom.* **31** 301–8

[9] Li H, Xu M and Zhu J 2019 headspace gas monitoring of gut microbiota using targeted and globally optimized targeted secondary electrospray ionization mass spectrometry *Anal. Chem.* **91** 854–63

[10] Zamora D, Amo-Gonzalez M, Lanza M, Fernández de la Mora G and Fernández de la Mora J 2018 Reaching a vapor sensitivity of 0.01 parts per quadrillion in the screening of large volume freight *Anal. Chem.* **90** 2468–74

[11] Li H and Zhu J 2018 Differentiating antibiotic-resistant staphylococcus aureus using secondary electrospray ionization tandem mass spectrometry *Anal. Chem.* **90** 12108–15

[12] Aernecke M J, Mendum T, Geurtsen G, Ostrinskaya A and Kunz R R 2015 Vapor pressure of hexamethylene triperoxide diamine (HMTD) estimated using secondary electrospray ionization mass spectrometry *J. Phys. Chem.* A **119** 11514–22

[13] Zhu J and Hill J E 2013 Detection of Escherichia coli via VOC profiling using secondary electrospray ionization-mass spectrometry (SESI-MS) *Food Microbiol.* **34** 412–7

[14] Bean H D, Zhu J and Hill J E 2011 Characterizing bacterial volatiles using secondary electrospray ionization mass spectrometry (SESI-MS) *J. Vis. Exp.* **52** e2664

[15] Dillon L A, Stone V N, Croasdell L A, Fielden P R, Goddard N J and Paul Thomas C L 2010 Optimisation of secondary electrospray ionisation (SESI) for the trace determination of gas-phase volatile organic compounds *Analyst* **135** 306–14

[16] Steiner W E, Clowers B H, Haigh P E and Hill H H 2003 Secondary ionization of chemical warfare agent simulants: atmospheric pressure ion mobility time-of-flight mass spectrometry *Anal. Chem.* **75** 6068–76

[17] Wu C, Siems W F and Hill H H 2000 Secondary electrospray ionization ion mobility spectrometry/mass spectrometry of illicit drugs *Anal. Chem.* **72** 396–403

[18] Singh K D *et al* 2019 Standardization procedures for real-time breath analysis by secondary electrospray ionization high-resolution mass spectrometry *Anal. Bioanal. Chem.* **411** 4883–98

[19] Malaskova M, Henderson B, Chellayah P D, Ruzsanyi V, Mochalski P, Cristescu S M and Mayhew C A 2019 Proton transfer reaction time-of-flight mass spectrometric measurements of volatile compounds contained in peppermint oil capsules of relevance to real-time pharmacokinetic breath studies *J. Breath Res.* **13** 046009

[20] Kessner D, Chambers M, Burke R, Agus D and Mallick P 2008 ProteoWizard: open source software for rapid proteomics tools development *Bioinformatics* **24** 2534–6

[21] Heaney L M, Ruszkiewicz D M, Arthur K L, Hadjithekli A, Aldcroft C, Lindley M R, Thomas C P, Turner M A and Reynolds J C 2016 Real-time monitoring of exhaled volatiles using atmospheric pressure chemical ionization on a compact mass spectrometer *Bioanalysis* **8** 1325–36

[22] Benjamini Y and Hochberg Y 1995 Controlling the false discovery rate: a practical and powerful approach to multiple testing *J. R. Stat. Soc.* **57** 289–300

[23] Kind T and Fiehn O 2007 Seven golden rules for heuristic filtering of molecular formulas obtained by accurate mass spectrometry *BMC Bioinf.* **8** 105

[24] Beigi M, Torki-Harchegani M and Ghasemi Pirbalouti A 2018 Quantity and chemical composition of essential oil of peppermint (Mentha × piperita L.) leaves under different drying methods *Int. J. Food Prop.* **21** 267–76

[25] Ragonese C, Sciarrone D, Grasso E, Dugo P and Mondello L 2016 Enhanced resolution of Mentha piperita volatile fraction using a novel medium-polarity ionic liquid gas chromatography stationary phase *J. Sep. Sci.* **39** 537–44

[26] Schmidt L and Goen T 2017 R-Limonene metabolism in humans and metabolite kinetics after oral administration *Arch. Toxicol.* **91** 1175–85

[27] Martínez-Lozano P, Rus J, Fernández de la Mora G, Hernández M and Fernández de la Mora J 2009 Secondary electrospray ionization (SESI) of ambient vapors for explosive detection at concentrations below parts per trillion *J. Am. Soc. Mass Spectrom.* **20** 287–94

[28] Kendrick E 1963 A mass scale based on $CH_2 = 14.0000$ for high resolution mass spectrometry of organic compounds *Anal. Chem.* **35** 2146–54

[29] Lan J, Gisler A, Bruderer T, Sinues P and Zenobi R 2020 Monitoring peppermint washout in the breath metabolome by secondary electrospray ionization-high resolution mass spectrometry *J. Breath Res.* accepted (https://doi.org/10.1088/1752-7163/ab9f8a)